Supplement of Atmos. Chem. Phys., 22, 5685–5700, 2022
https://doi.org/10.5194/acp-22-5685-2022-supplement

Supplement of

Chemical transformation of α-pinene-derived organosulfate via heterogeneous OH oxidation: implications for sources and environmental fates of atmospheric organosulfates

Rongshuang Xu et al.

Correspondence to: Jian Zhen Yu (jian.yu@ust.hk) and Man Nin Chan (mnchan@cuhk.edu.hk)

1. Experimental Details

The heterogeneous OH oxidation of αpOS-249 aerosols was conducted using an OFR with a volume of ~ 13 L (18-inch length, 8-inch inner diameter) at 50 ± 2.0 % RH and 298.0 ± 0.5 K. As shown in **Scheme S1**, aqueous αpOS-249 aerosols were first generated by passing its solution through a constant output atomizer (TSI Model 3076) using 3 L min^{-1} of nitrogen (N_2). Before entering the reactor, the aerosols were directly mixed with dry/wet nitrogen (N_2), oxygen (O_2) and ozone (O_3) to make up a total flow of ~ 5 L min^{-1}, corresponding to a residence time of ~ 156 s. The relative humidity (RH) inside the reactor was maintained by varying the mixing ratio of dry and humidified N_2. The RH and temperature were measured by a RH-temperature sensor (Vaisala, HM40).

Inside the reactor, OH was generated via photolysis of O_3 with UV light at 254nm in the presence of water vapor. The O_3 was generated by passing O_2 through an O_3 generator (ENALY 1000BT-12). The concentration of gas-phase OH radical was varied by changing the O_3 concentrations, monitored by an O_3 analyzer (2B technologies, Model 202). The OH exposure, a product of gas-phase OH radical concentration and the residence time, ranged from 0–17.4 × 10^{11} molecule cm^{-3} s and was determined by measuring the decay of sulfur dioxide (SO_2) (Teledyne SO_2 analyzer, Model T100) in independent calibrating experiments in the absence of αpOS-249 aerosols based on the reaction rate between gas-phase OH radicals and SO_2 (= 9.0 × 10^{-13} $molecule^{-1}$ cm^3 s^{-1}) at 298 K (Kang et al., 2007). Furthermore, SO_2 calibration experiments in the presence of αpOS-249 aerosol were also conducted to investigate the effects of the aerosols on the generation and concentration of gas-phase OH radicals inside the reactor. A variation of ~10 % in the determination of OH exposure was observed over the experimental conditions.

The aerosol stream leaving the reactor then passed through an annular Carulite catalyst denuder (manganese dioxide/copper oxide catalyst; Carus Corp.) and an activated charcoal denuder to remove residual O_3 and other gas-phase species. 3 L min^{-1} of the stream was sampled onto the Teflon filters (2.0 μm pore size, Pall Corporation) by an air sampling pump (Gilian 500, Sensidyne) for 30 min, with a total gas sampling volume of ~ 90 L. Duplicate filters were collected from each of oxidation experiments for subsequent chemical analysis. After collection, filters were immediately stored at −20 °C in the dark and analysed within 3 months.

Part of the remaining stream was introduced into a scanning mobility particle sizer (SMPS, TSI, CPC Model 3775, Classifier Model 3081) to measure the size distribution of aerosols. The size distribution was sampled from 16 to 604.3 nm and scans were repeated every 180 s (sheath flow of 3 L min^{-1}). The aerosol mass loading was determined from measured volume concentration assumed for spherical aerosols with a unit density as a lower limit as sodium salts of the organosulfates (R−OSO_3Na) usually have the density larger than 1.0 g cm^{-3} (e.g. 1.60 g cm^{-3} of CH_3SO_4Na; 1.46 g cm^{-3} of $C_2H_5SO_4Na$; Chemistry Dashboard). Before oxidation, the mean surface weighted diameter for aerosol distribution was about 181 ± 0.5 nm with a geometric standard deviation of 1.3 and the aerosol mass loading was measured to be ~2000 μg m^{-3}.

The OFR was designed with a small surface-to-volume ratio to minimize the aerosol wall loss (Kang et al., 2007; Lambe et al., 2011). The aerosol transmission efficiency for aerosol diameter larger than 150 nm was reported to be greater than 80% (Lambe et al., 2011). In our study, the wall loss was expected to be small as the aerosol diameter was measured to be 181.3 ± 0.5 nm and the aerosols with a diameter larger than 150 nm accounted for a significant fraction of total aerosol number and mass. This wall loss factor was thus not corrected in the calculations. However, we expect this would not significantly affect the determination of reaction kinetics (i.e. k) and inorganic sulfate yield. This is because concentration ratios (e.g. I/I_0) were used and the effect of wall loss would be cancelled out in the calculations.

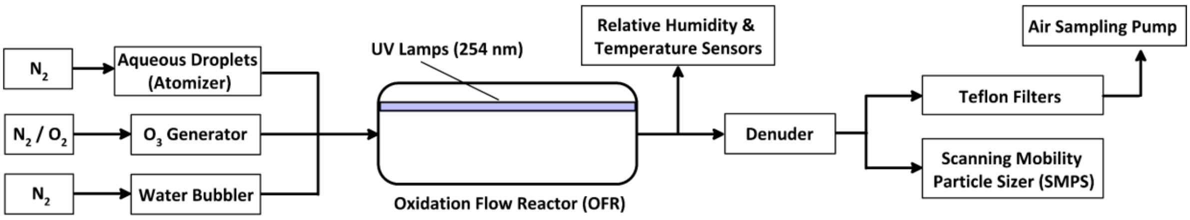

Scheme S1. Schematic diagram for experimental setup of the heterogeneous OH oxidation.

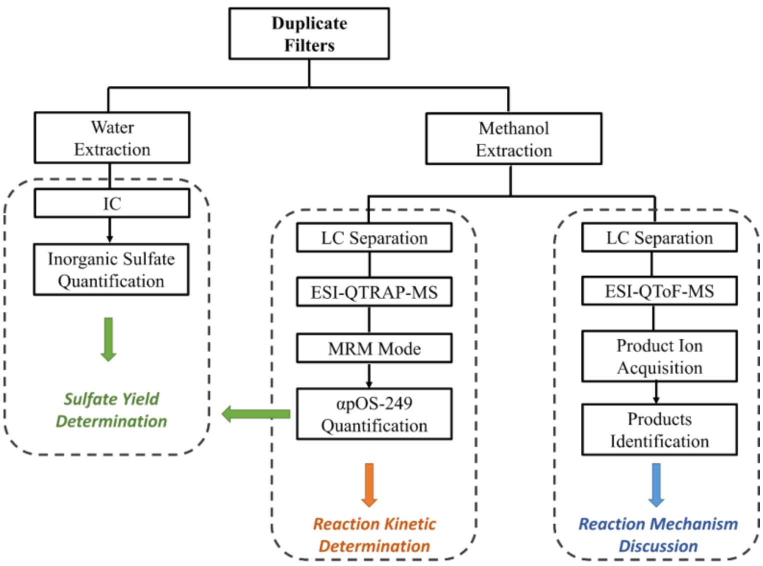

Scheme S2. An overview of the chemical analysis performed in this work.

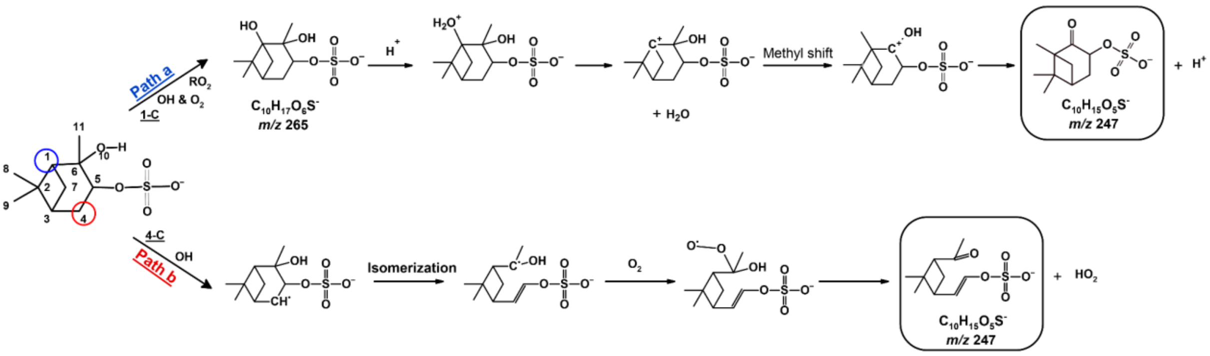

Scheme S3. Possible formation mechanisms for *m/z* = 247 ($C_{10}H_{15}O_5S^-$) ion.

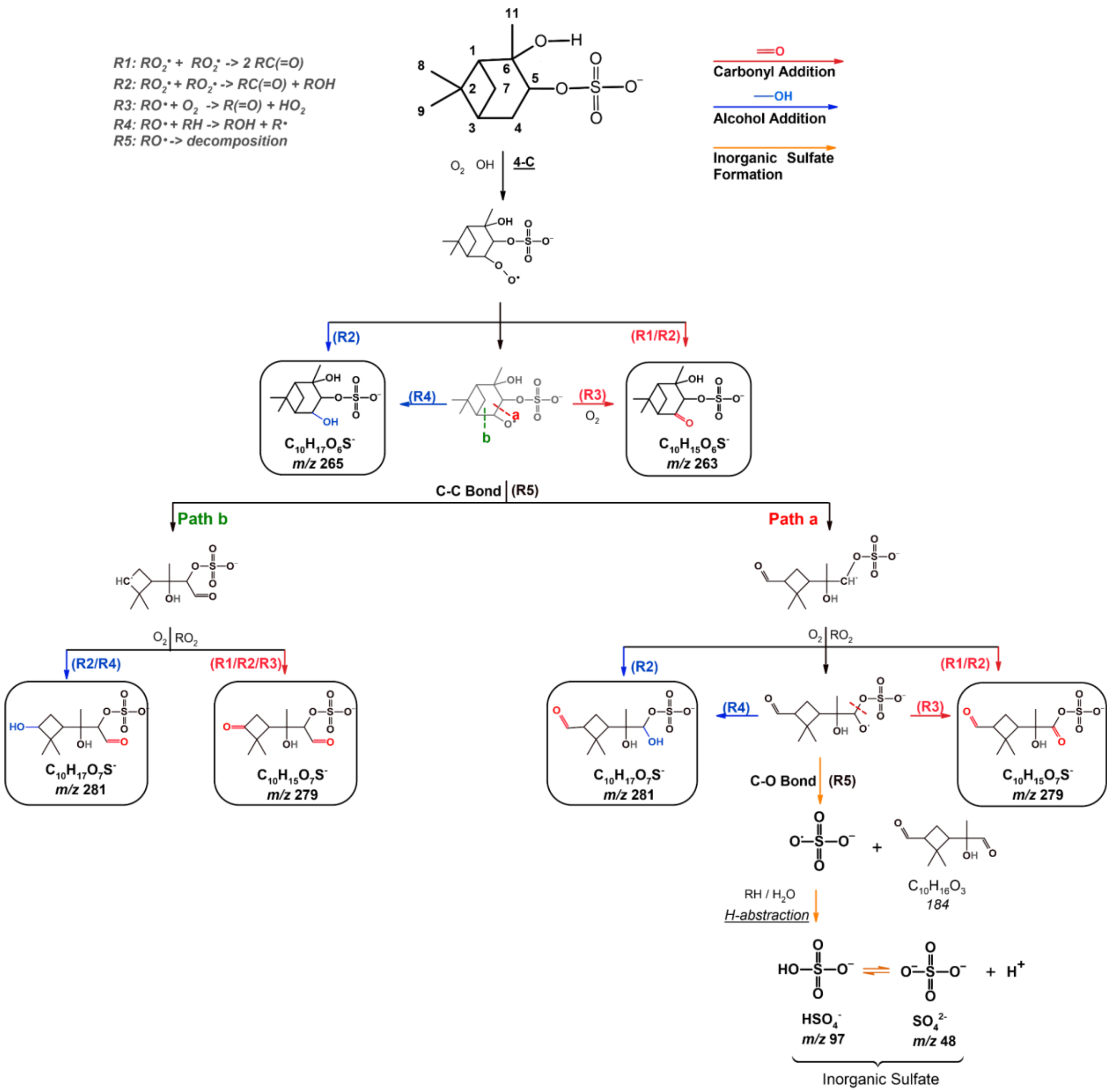

Scheme S4. Formation mechanisms tentatively proposed for the formation of more oxygenated OSs (*m/z* = 279 and 281) and inorganic sulfates involving the decomposition of alkoxy radicals.

Table S1. MS parameters of MRM transition for quantifying αpOS-249.

Analyst	Products ion	Mass transition	DP [a] (volts)	EP [b] (volts)	CE [c] (volts)	CXP [d] (volts)	MDL [e] (ng/mL)	LOQ [e] (ng/mL)
αpOS-249	HSO_4^-	249/97	-95.51	-7.79	-37.34	-14.97	2.95	9.82
D_{17}-octyl sulfate	HSO_4^-	225/97	-83.46	-9.05	-25.97	-5.98	-	-

[a]DP: declustering potential., [b] EP: entrance potential., [c] CE: collision energy, [d] CXP: collision cell exit potential. [e] Method detection limit defined as 3-fold standard deviation of 10 ng/mL standard solution signals and limit of quantification defined as 10-fold standard deviation of 10 ng/mL standard solution signals. And these values were obtained by Wang et al. (2017) using the same instrument and similar detection conditions.

Table S2. The hydrogen abstraction rate for different reaction sites of αpOS-249 predicted by the SAR model developed by Monod and Doussin (2008)*.

Name	αpOS-249	
Chemical structure	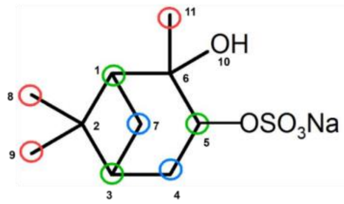	
	Reaction site	Rate ($\times 10^{-13}$ cm^3 $molecule^{-1}$ s^{-1})
Primary carbon	8-C	7.50
	9-C	7.50
	11-C	2.82
Secondary carbon	4-C	18.00
	7-C	14.63
Tertiary carbon	1-C 3-C 5-C	6.99 17.20 1.29
Hydroxyl (-OH) group	10-O	1.48

* It is noted that the SAR model does not include the parameterization of sulfate group. As a first approximation, the effect of sulfate group on the reactivity is evaluated using the descriptor of carboxylate anion (COO^-).

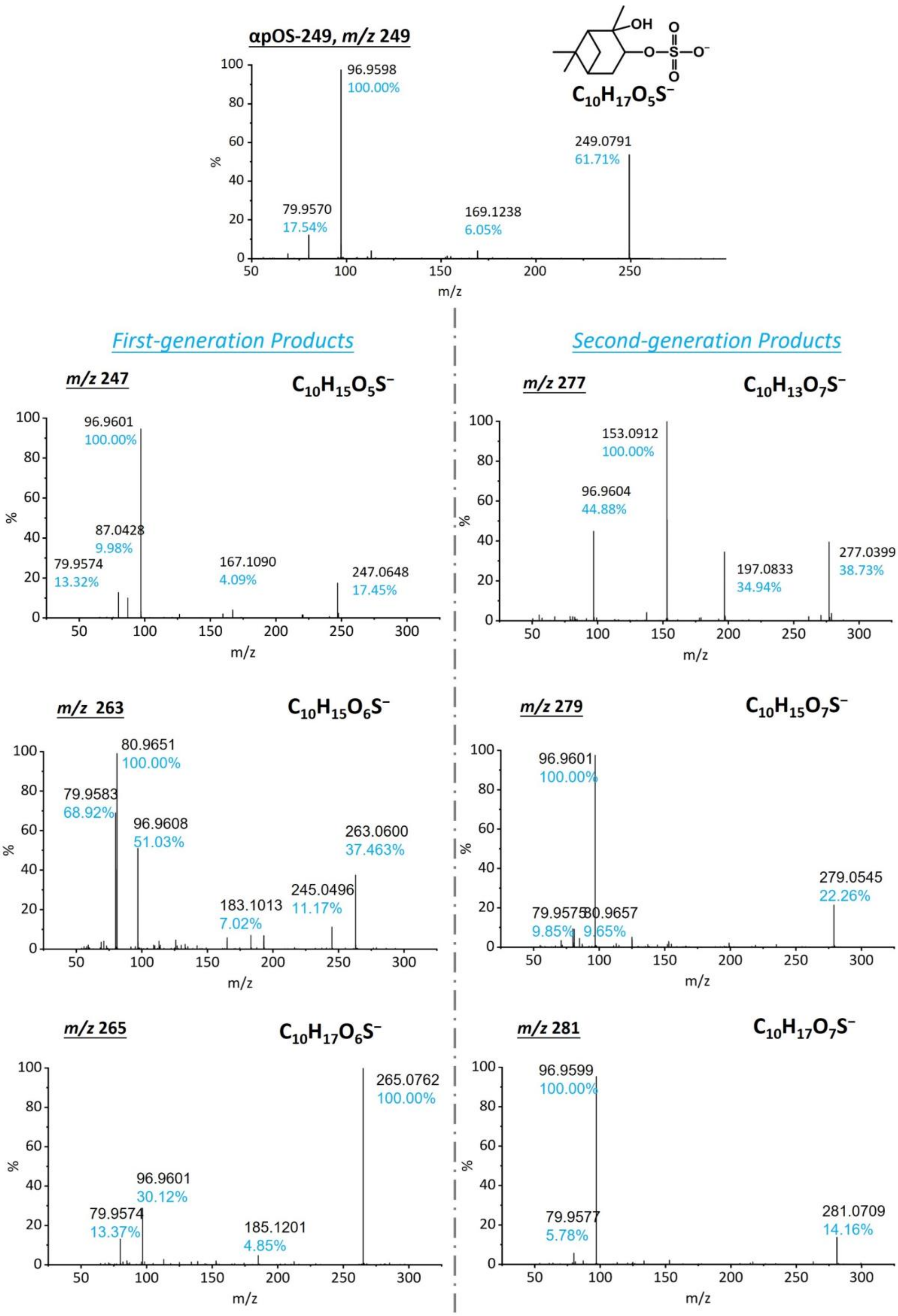

Figure S1. MS^2 spectrum for αpOS-249 and reaction products in the HPLC/ESI-QToF-MS/MS measurements.

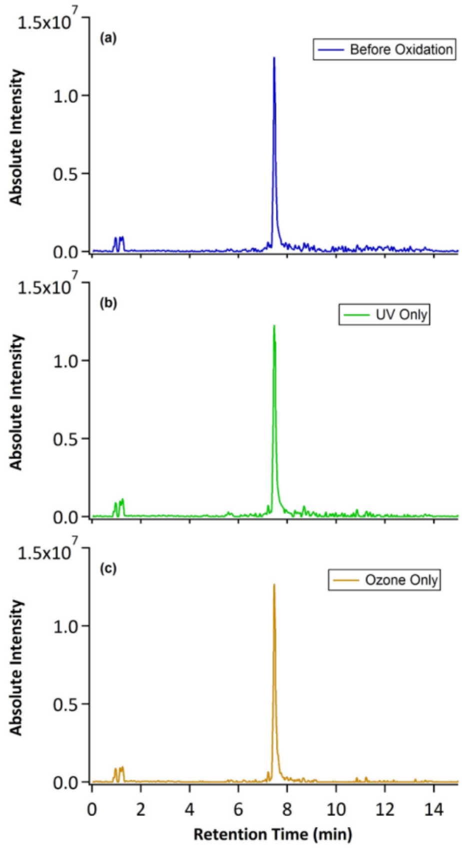

Figure S2. The total ion chromatograms (TICs) of αpOS-249 aerosols characterized by the HPLC/ESI-QToF-MS to examine the effects of UV light and ozone on αpOS-249 in control experiments.

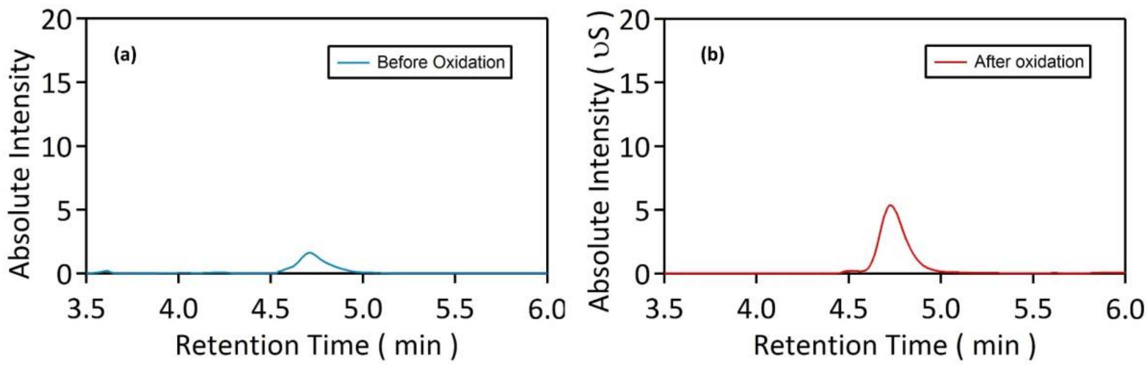

Figure S3. The ion chromatograms before (a) and after (b) heterogeneous OH oxidation of αpOS-249.

2. Determination of measurement uncertainties:

2.1 The uncertainty for the quantification of αpOS-249 ($C_{10}H_{17}O_5S^-$) and sulfate (SO_4^{2-}) ion

Measurement precisions for the concentration of species *i* (σ_{Ci}) are propagated from precisions of volumetric measurements, chemical composition measurements, and blank sample variability and sample repeatability referring to Bevington et al. (1993), and Williams et al. (2012). For simplicity, the following equations are used to calculate the uncertainty associated with our filter-based measurements:

$$C_i = \frac{M_i - B_i}{V} \quad (1)$$

$$B_i = \frac{1}{n}\sum_{j=1}^{n} B_{ij} \;\; for\; B_i > \sigma_{B_i} \quad (2)$$

$$B_i = 0 \; for\; B_i \le \sigma_{B_i} \quad (3)$$

$$\sigma_{B_i} = STD_{B_i} = [\frac{1}{n-1}\sum_{j=1}^{n}(B_{ij} - B_i)^2]^{\frac{1}{2}} \;\; for\; STD_{B_i} > SIG_{B_i} \quad (4)$$

$$\sigma_{B_i} = STD_{B_i} = [\frac{1}{n}\sum_{j=1}^{n}(\sigma_{B_{ij}})^2]^{\frac{1}{2}} \;\; for\; STD_{B_i} \le SIG_{B_i} \quad (5)$$

$$\frac{\sigma_V}{V} = 0.05 \quad (6)$$

$$\sigma_{C_i} = [\frac{{\sigma_{M_i}}^2 + {\sigma_{B_i}}^2}{V^2} + \frac{{\sigma_V}^2 (M_i - B_i)^2}{V^4}]^{\frac{1}{2}} \quad (7)$$

where

B_i = average amount of species *i* on blank samples

B_{ij} = the amount of species *i* found on blank sample *j*

C_i = the concentration of species *i*

M_i = amount of species *i* on the substrate

n = total number of samples in the sum

SIG_{Bi} = the root mean square error (RMSE), the square root of the averaged sum of the squared σ_{Bij}

STD_{Bi} = standard deviation of the blank samples

σ_{Bi} = blank precision for species *i*

σ_{Bij} = precision of the species *i* found on blank sample *j*

σ_{Ci} = propagated precision for the concentration of species *i*

σ_{Mi} = precision of amount of species *i* on the substrate

σ_V = precision of sample volume

V = sample volume

The precisions (σ_{Mi}) were determined from duplicate analysis of samples. When duplicate sample analysis is made, the range of results, *R*, is nearly as efficient as the standard deviation since two measures differ by a constant ($1.128\sigma_{Mi} = R$). Based on the blank samples and duplicate samples, coefficients needed for determining uncertainty are given in following table:

Species	Quantification method	No. of Blanks	No. of duplicate standard	Blank Precision (σ_{Bi}, mg)	Duplicate Precision (σ_{Mi}, mg)
αpOS-249	HPLC/ESI-QTRAP-MS	3	3	0.0023	0.0216
Sulfate and/or bisulfate	IC	3	3	0.0019	0.0017

2.2 The uncertainty for the yield, $\boldsymbol{\sigma_{yield_j}}$

$$\sigma_{yield_j} = [\frac{{\sigma_{\alpha\mathrm{pOS-249}_j}}^2 + {\sigma_{\alpha\mathrm{pOS-249}_0}}^2}{(\alpha\mathrm{pOS} - 249_0 - \alpha\mathrm{pOS} - 249_j)^2} + \frac{{\sigma_{sulfate_j}}^2 + {\sigma_{sulfate_0}}^2}{(sulfate_j - sulfate_0)^2}]^{\frac{1}{2}} * yield_j$$

where

σ_{yield_j}= precision of molar yield on sample *j*

$\sigma_{\alpha\mathrm{pOS-249}_j}$= precision of αpOS-249 on sample *j*

$\sigma_{\alpha\mathrm{pOS-249}_0}$= precision of αpOS-249 on first sample (prior to oxidation)

$\sigma_{sulfate_j}$= precision of sulfate on sample *j*

$\sigma_{sulfate_0}$= precision of sulfate on first sample (prior to oxidation)

$\alpha\mathrm{pOS} - 249_0$= the amount of αpOS-249 on first sample (prior to oxidation)

$\alpha\mathrm{pOS} - 249_j$= the amount of αpOS-249 on sample *j*

$yield_j$= molar yield for sample *j*

2.3 The uncertainty for OH exposure, $\boldsymbol{\sigma_{exp}}$

$$\sigma_{exp} = 0.005\ (OH\ exposure)\sqrt{\left(16 + \frac{2}{(OH\ exposure \times k_{SO_2})^2}\right)}$$

where 0.005 is the precision of SO_2 analyzer (0.5 % of the reading), k_{SO_2} is the second-order rate constant of the gas-phase OH and SO_2 reaction: 9×10^{-13} cm^3 $molecule^{-1}$ s^{-1}.

2.4 The uncertainty for parent decay index, $\boldsymbol{\sigma_{\frac{I}{I_0}}}$

$$\sigma_{\frac{I}{I_0}} = \frac{I}{I_0} \times \sqrt{\left(\frac{\sigma_I}{I}\right)^2 + \left(\frac{\sigma_{I_0}}{I_0}\right)^2}$$

where *I* is the concentration of αpOS-249 at a given OH exposure, I_0 is the concentration of αpOS-249 before oxidation, σ_I is the uncertainty of αpOS-249 on sample at a given OH exposure.

2.5 The uncertainty for atmospheric lifetime, $\boldsymbol{\sigma_\tau}$

$$\sigma_\tau = \tau\sqrt{\left(\frac{\sigma_k}{k}\right)^2}$$

where *k* is the fitted heterogeneous OH rate constant.

References

Bevington, P. R., Robinson, D. K., Blair, J. M., Mallinckrodt, A. J., and McKay, S.: Data reduction and error analysis for the physical sciences, Computers in Phys., 7, 415−416 https://doi.org/10.1063/1.4823194, 1993.

Ellison, S. L. R. and Williams, A. (Eds.): Eurachem/CITAC guide: quantifying uncertainty in analytical measurement, 3rd Edition, ISBN 13: 9780948926303, available from www.eurachem.org, 2012.

Kang, E., Root, M. J., Toohey, D. W., and Brune, W. H.: Introducing the concept of Potential Aerosol Mass (PAM), Atmos. Chem. Phys., 7, 5727–5744, https://doi.org/10.5194/acp-7-5727-2007, 2007.

Lambe, A. T.; Ahern, A. T.; Williams, L. R.; Slowik, J. G.; Wong, J. P. S.; Abbatt, J. P. D.; Brune, W. H.; Ng, N. L.; Wright, J. P.; Croasdale, D. R.; Worsnop, D. R.; Davidovits, P.; Onasch, T. B.: Characterization of aerosol photooxidation flow reactors: heterogeneous oxidation, secondary organic aerosol formation and cloud condensation nuclei activity measurements, Atmos. Meas. Tech., 4, 445−461, https://doi.org/10.5194/amt-4-445-2011, 2011.

Monod A. and Doussin, J. F.: Structure-activity relationship for the estimation of OH-oxidation rate constants of aliphatic organic compounds in the aqueous phase: alkanes, alcohols, organic acids and bases, Atmos. Environ., 42, 7611–7622, https://doi.org/10.1016/j.atmosenv.2008.06.005, 2008.

Wang, Y., Ren, J., Huang, X. H. H., Tong, R., and Yu, J. Z.: Synthesis of four monoterpene-derived organosulfates and their quantification in atmospheric aerosol samples, Environ. Sci. Technol., 51, 6791−6801, https://doi.org:10.1021/acs.est.7b01179, 2017.